https://doi.org/10.1142/9789811280184_0015

Chapter 15

Higgs Physics at HL-LHC

Aleandro Nisati

Istituto Nazionale di Fisica Nucleare, Sezione di Roma, P.le A. Moro 2, Rome, 00185, Italy

Vivek A. Sharma

Department of Physics, University of California San Diego, 9500 Gilman Drive, La Jolla, CA 92093-0319, USA

In this chapter we review the projected reach of the ATLAS and the CMS upgraded detectors with full HL-LHC dataset of about 3000 fb^{-1} at $\sqrt{s} = 14$ TeV (per experiment)in the measurement of key properties of the Higgs boson such as its mass and natural width, coupling to SM fermions and bosons, and its self-coupling.

1. Introduction

The discovery[1,2] of the Higgs boson (H) represents a major milestone in the understanding of the Electroweak Symmetry Breaking mechanism (EWSB) in nature. Since its discovery, a major push at the LHC has been to determine whether this object is the elementary boson predicted by the Standard Model (SM) of particle physics, or whether it represents the first observation of a beyond SM (BSM) particle. With the first ≈ 140 fb^{-1} of p-p collisions at the LHC taken mainly at $\sqrt{s} = 13$ TeV, an impressive set of Higgs boson properties, including its spin-parity have been measured. The Higgs boson mass, a free parameter in the theory, has been measured with better than per mille accuracy. The Higgs mass of ≈ 125 GeV allows for measurements of its coupling to a variety of fermions. Its coupling to gauge bosons and the heavy fermions of the third generation has been measured

with a precision of $\approx 5\%$ and 10% respectively. All the major Higgs boson production modes have been observed and the first evidence of its coupling to muons has been established.

While a general portrait[3–5] of the Higgs boson has emerged, the experimental exploration of the Higgs sector is in its infancy. With about $20\times$ more data that HL-LHC is expected to deliver at $\sqrt{s} = 14$ TeV, the two major thrusts in Higgs physics are on (i) measurement of its mass, natural width and precise measurements of its couplings to fermions and bosons (ii) the first measurements of Higgs self-interaction.

The motivation for precision coupling measurement stems from the fact that rates for Higgs-related processes could be impacted by the contributions of BSM particles which may be too heavy to be directly produced at the LHC but still contribute to its properties via quantum loops. A suggested rule of thumb[6] is that increasing the coupling precision by a factor of four doubles the BSM mass scale that can be indirectly probed. The second important line of HL-LHC probe is on the shape of the Higgs potential. After EWSB, the Higgs potential gives rise to cubic and quartic terms in the Higgs boson field, resulting in a self-coupling term. Given a precise Higgs boson mass, this self-coupling is precisely predicted in the SM and can be measured in Higgs boson pair production (HH) processes. Any significant deviation from SM predictions signifies BSM physics and has major consequences for our understanding of this universe.

This chapter is organised as follows: The ATLAS and CMS detector upgrade for HL-LHC is summarised in Sec. 2, followed by a brief description of the procedures used for the projections in Sec. 3. Section 4 projects the precision on measurements of Higgs mass and its natural width, Sec. 5 summarizes the Higgs boson couplings measurements prospects. Section 6 is dedicated to the HL-LHC potential for the measurements of Higgs self-coupling, followed by a summary in Sec. 7.

2. Upgraded ATLAS and CMS detectors for the HL-LHC

In order to operate in the high intensity environment of the HL-LHC, ATLAS[7] and CMS[8] experiments are planning significant modification of their detectors, see Chapters 11 and 12 for a summary.[9] These upgrades, with increased granularity detectors with larger acceptances, targets efficient data taking and event reconstruction at increased luminosity and pileup (PU), up to $\sim$200 additional inelastic interactions per bunch crossing and up to an order of magnitude larger radiation doses. For both detectors, in order to

maintain or even lower the trigger thresholds with respect to Run 2, several trigger subsystems will be replaced or upgraded as well. New charged particle tracking systems will be installed, extending the tracking coverage up to pseudo-rapidities of $|\eta| = 4$. The addition of new timing detectors with a precision of about 35 ns, covering up to $|\eta| = 3$ for CMS and $2.4 \leq |\eta| \leq 4.0$ for ATLAS, will introduce new PU rejection capabilities in the HL-LHC environment. The existing ATLAS Liquid Argon and Tile calorimeters as well as the CMS barrel electromagnetic and hadron calorimeters will be upgraded with new electronics. The CMS endcap electromagnetic and hadron calorimeters will be replaced with a new high-granularity sampling calorimeter. Finally, the muon systems of ATLAS and CMS will be upgraded with fast electronics to deal with the extreme rates of secondary particles produced in HL-LHC collisions and additional muon chambers will be added to increase acceptance and redundancy.

3. Prognostication on Higgs studies in the HL-LHC era

As Niels Bohr once said, "Prediction is very difficult, especially if it's about the future!". We need to keep these sage words in mind while prognosticating the future. The ATLAS and CMS Collaborations have followed a few conservative strategies to project the precision of the Higgs measurements with the data collected at the end of HL-LHC era. The majority of the Higgs boson studies presented in this chapter generally follow the techniques used in Run 2 analyses. In some cases, the Run 2 analyses have been extrapolated to HL-LHC, taking into account the superior performance expected from the upgraded ATLAS and CMS apparatuses, and the large event pile-up expected at the HL-LHC. In other cases, such as for Higgs self-coupling measurements, Monte Carlo simulation studies were performed to assess the physics prospects at HL-LHC.

The expected performance at HL-LHC depends on both the signal event statistics, as well as on the systematic uncertainties that affect the event reconstruction in the unprecedented pile-up produced in the p-p collisions. Several scenarios have been identified to describe the impact of these uncertainties on the measurements. In the baseline scenario, the systematic uncertainties are set according to the technical recommendations[10] for HL-LHC projections. The expected uncertainty on the integrated luminosity of the full HL-LHC dataset is assumed to be 1%, lower than the Run 2 uncertainty of 1.7%. Theoretical systematic uncertainties are reduced by a factor of two with respect to those used in the Run 2 analyses, under the

assumption of continued progresses on theoretical computations of perturbative corrections, PDFs, α_s etc. The statistical components of the experimental uncertainties are scaled according to $1/\sqrt{L}$.

In terms of analysis tools, the rapid deployment of Deep Machine Learning methods in Higgs measurements is expected to bring substantial gains in the HL-LHC era. Finally, it should be noted that in general, at particle colliders, due to continued innovations in analysis techniques, the precision in the final measurements of an electroweak observable have by far exceeded their prior projections.

4. Mass and natural width

The Higgs boson mass, m_H, is an unknown parameter of the Standard Model which should be measured as precisely as possible. The Higgs boson mass, together with the top quark mass, impacts the electroweak vacuum stability, and it has important consequences in cosmology.

With the Run 2 data, the Higgs boson mass, m_H, has been measured to be $m_H = 124.97 \pm 0.24$ GeV (ATLAS[11]) and $m_H = 125.38 \pm 0.14$ GeV (CMS[12]). These are the result of the combination of the independent $H \to ZZ^{(*)} \to 4l$ and $H \to \gamma\gamma$ mass measurements in each experiment.

At HL-LHC, the mass measurement accuracy will be limited by the systematic uncertainties dominated by the uncertainty on the electron, photon and muon energy scales. The projection studies assumed (conservatively) that the energy scale achieved in Run 2, namely 0.01% (0.15%) for the muon (electron), holds for HL-LHC as well. Consequently, the accuracy on the Higgs mass measurement will be dominated by the 4-lepton final states, particularly the $H \to ZZ^{(*)} \to \mu\mu\mu\mu$ final state, which are statistically limited in the current measurements. In the $H \to ZZ^{(*)} \to \mu\mu\mu\mu$ channel, an overall systematic uncertainty of 15 MeV is projected for the m_H measurement. In the $H \to ZZ^{(*)} \to \mu\mu ee$ and $H \to ZZ^{(*)} \to eeee$ channels, the m_H measurements are less precise, with a total uncertainty of about 100 MeV. A statistical accuracy of about 28 MeV is expected with 3000 fb^{-1} from the $H \to ZZ^{(*)} \to \mu\mu\mu\mu$ channel, that reduces to 22 MeV when combined with the other 4-lepton final states. Finally, by combining all $H \to ZZ^{(*)} \to 4l$ final states, a total uncertainty of 30 MeV on m_H is projected for the HL-LHC data set.

The total width (Γ_H) is another very important Higgs boson observable for probing new physics contributions. In the SM, the Higgs boson width is predicted to be 4.1 MeV for $m_H = 125$ GeV. The invariant mass

resolution of the two Higgs final states that can be fully reconstructed ($H \to \gamma\gamma$ and $H \to ZZ^{(*)} \to 4l$) is much larger ($O(1$ GeV)) than the SM prediction, therefore only a model-independent experimental upper limit can be set. The projected upper limits at 95% C.L. of the Higgs boson width are 94 MeV (statistical uncertainty only) and 177 MeV (statistical and systematic uncertainties combined).

More precise (but model-dependent) estimates of Γ_H can be obtained by relating its off-shell production to its on-shell production.[13–16] With Run 2 data, CMS measurement of the Higgs boson off-shell production processes $H \to ZZ^{(*)} \to 4l$ and $H \to ZZ^{(*)} \to 2l2\nu$ yield $\Gamma_H = 3.2^{+2.4}_{-1.7}$ MeV.[17] A measurement[18] by ATLAS yields $\Gamma_H = 4.6^{+2.6}_{-2.5}$ MeV. The observed (expected) upper limit on the total width is 9.7(10.2) MeV at 95% confidence level in the asymptotic approximation. With this method and by combining the CMS and ATLAS results with the HL-LHC data, a precision on the Higgs boson width of about 0.8 MeV, dominated by theoretical uncertainties, can be obtained.

5. The Higgs boson production, decay and couplings

The leading Feynman diagrams for Higgs boson production in pp collisions at the LHC, decay and pair production are shown in Fig. 1.

5.1. *Production and Decay*

The projected precision in the measurements of various production modes are shown in Fig. 2(left). The expected precision ranges from 1.6% (ggH) to 5.7% (VH) and begins to be dominated by the theoretical uncertainties within the phase space of the experimental measurement. The major Higgs decay rate measurements should reach precision of about 3% for $H \to \gamma\gamma$, $H \to ZZ^{(*)}$, $H \to WW^{(*)}$ and $H \to \tau\tau$, and 4% for ($H \to b\bar{b}$). They are all expected to be dominated by theoretical uncertainties. The measurements of rare decays $H \to \mu^+\mu^-$ and $Z\gamma$ will be statistically limited with a branching ratio uncertainty of about 8% and 19% respectively.

5.2. *Higgs Boson Couplings to bosons and fermions*

BSM phenomena are expected to affect the Higgs production modes and its decay channels in a correlated way if they are governed by similar interactions. Any modification in the interaction between the Higgs boson and, e.g. the W bosons and top quarks would not only affect the $H \to WW^{(*)}$

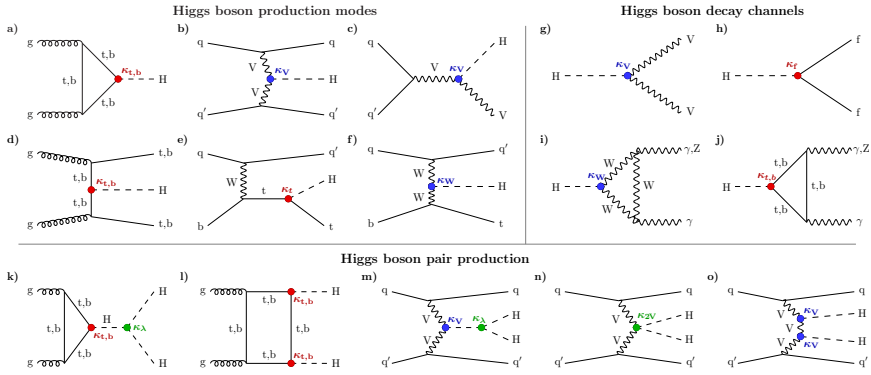

Fig. 1. Feynman diagrams for the leading order Higgs boson interactions: Higgs boson production in (a) gluon-gluon fusion ($gg \to H$), (b) vector boson fusion (VBF), (c) associated production with a W or Z (V) boson (VH), (d) associated production with a top or bottom quark pair (ttH or bbH), (e, f) associated production with a single top quark (tH); with Higgs boson decays into (g) heavy vector boson pairs, (h) fermion-antifermion pairs, and (i, j) photon pairs or $Z\gamma$; Higgs boson pair production: (k, l) via gluon-gluon fusion, and (m, n, o) via vector boson fusion. The different Higgs boson interactions are labelled with the coupling modifiers κ, and highlighted in different colours for Higgs-fermion interactions (red), Higgs-gauge-boson interactions (blue), and multiple Higgs boson interactions (green).[3]

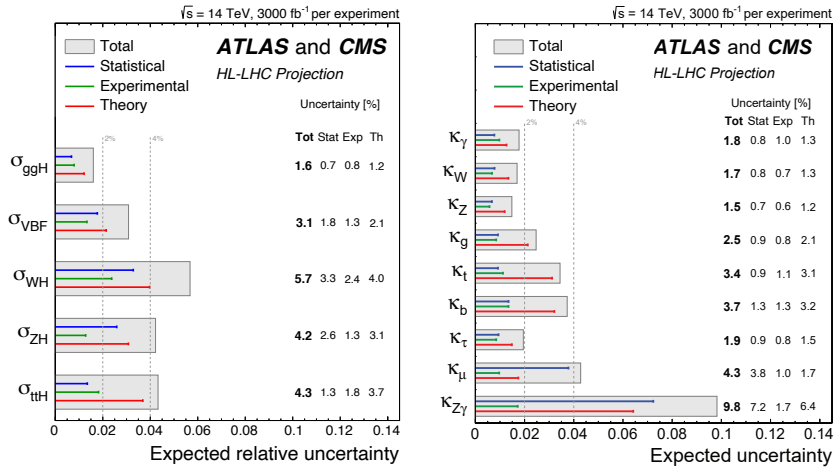

Fig. 2. (Left) projected precision in Higgs production cross section measurement, (right) projected precision in the modifiers of Higgs coupling to bosons and fermions.

and $H \to \gamma\gamma$ decay rates but also the production cross-section for gluon fusion production process ggH, VBF and VH. In order to probe small

contribution of BSM particles to the SM predictions, the κ-framework[19] developed to analyse Run 2 data is used. For a given production process or decay mode j, a coupling modifier κ_j is defined such that;

$$\kappa_j^2 = \sigma_j/\sigma_j^{\rm SM} \quad \text{or} \quad \kappa_j^2 = \Gamma^j/\Gamma^j_{\rm SM}. \tag{1}$$

In the SM, all κ_j values are positive and equal to unity. Six coupling modifiers κ_W, κ_Z, κ_t, κ_b, κ_τ and κ_μ corresponding to tree-level Higgs couplings are introduced along with effective coupling modifiers κ_g, κ_γ and $\kappa_{Z\gamma}$ addressing the loop-process in ggH, $H \to \gamma\gamma$ and $H \to Z\gamma$. The total width of the Higgs boson, relative to the SM prediction, varies with the coupling modifiers as $\Gamma_H/\Gamma_H^{\rm SM} = \sum_j {\rm B}^j_{\rm SM}\kappa_j^2/(1-{\rm B}_{\rm BSM})$, where ${\rm B}^j_{\rm SM}$ is the SM branching fraction for the $H \to jj$ channel and ${\rm B}_{\rm BSM}$ is the Higgs boson branching fraction to BSM final states. In the results for the κ_j parameters presented here ${\rm B}_{\rm BSM}$ is fixed to zero and only decays to SM particles are allowed. The projected precision on Higgs boson coupling modifiers are shown in Fig. 2(right).

It should be noted that the κ framework merely compares the experimental measurement to their best values computed within the SM and does not require any BSM calculation. It is based on assumptions and has limitations in its ability to describe general deformations of the SM. A systematic and powerful way to capture the deviations in Higgs coupling due to BSM phenomena comes from SM Effective Field Theory[5] and are being studied in the context of HL-LHC.[20]

5.3. *Rare Higgs Decays*

A dataset of 3000 fb^{-1} will allow probe of several rare or hard-to-detect Higgs boson decays. Having measured Higgs boson coupling to the vector bosons and fermions of the third generation to $\approx 10\%$ precision, the attention will focus on measurements of Higgs boson coupling to the second and first generation fermions. So far, due to tiny rates and large backgrounds, there are no model-independent and sensitive strategies at LHC to directly measure the Higgs coupling to the first generation fermions. For example, the best 95% CL limit[21] on $H \to e^+e^-$ decay rate with Run 2 data is about 3×10^{-4} to be compared with the expected SM branching ratio of $\approx 5 \times 10^{-9}$. But by searching for and not finding such decays in the Run 2 data, we have learnt already that Higgs couplings to fermions are not universal.

5.3.1. $H \to \mu^+\mu^-$

At the HL-LHC, the relatively most accessible channel to probe Higgs coupling to the second generation is $H \to \mu^+\mu^-$. With a branching rate of 2×10^{-4} and an irreducible $Z/\gamma^* \to \mu^+\mu^-$ background with a rate several orders of magnitude higher, it is also one of the most difficult Higgs decay channels to probe. The $H \to \mu^+\mu^-$ signal appears as a narrow peak over a smoothly falling Drell-Yan background. The CMS detector, with an excellent charged particle momentum resolution of $\approx$ 1–2.5% and precise background shape modeling, reported[22] the first evidence-level measurement of this decay with the Run 2 data. After the phase II upgrade, CMS and ATLAS will benefit from the improved charged particle tracking acceptance and momentum resolution leading to improvement in $m_{\mu\mu}$ resolution (for example, the expected momentum resolution improvement in CMS is about 30%). These improvements will enable a direct measurement of κ_μ with an uncertainty of about 4%.[23]

5.3.2. $H \to c\bar{c}$

Due to small charm hadron masses and low charged particle multiplicity in their decay, the identification of charm quark jets in the multi-jet environment of LHC is difficult. This limitation, along with the contamination from b quark jets and the small decay rate of $H \to c\bar{c} \approx 3\%$ makes the direct measurement of Higgs coupling to charm very challenging. In the recent years, ML techniques have been employed to better isolate $H \to c\bar{c}$ signal from multitudes of backgrounds. At the HL-LHC, a 95% upper limit on the signal strength of VH($H \to c\bar{c}$) production mode of 6.4 times the SM prediction and a constraint of $|\kappa_c| < 3.0$ is projected.[24]

5.3.3. $H \to Z\gamma$

The SM Higgs boson can decay into $H \to Z\gamma$ through loop diagrams and the branching ratio is predicted to be $BR(H \to Z\gamma) \approx 1.5 \times 10^{-3}$. It is an interesting mode because the measured rate can differ from the SM prediction in many BSM scenarios.[25–27] Due to the small branching fraction in the SM, the $H \to Z\gamma$ decay has not yet been observed at the LHC. An upper limit[28] at 95% confidence level on the production cross-section times the branching ratio for $pp \to H \to Z\gamma$ has been set at 3.6 times the SM prediction. The extrapolation to HL-LHC uses simple scaling approach on the Run 2 analysis. The measurement is expected to be statistically limited.

For example, with the 3000 fb^{-1} dataset, ATLAS expects only a 5 standard deviations observation of this mode and a signal strength measurement of 23% precision.[20] The effective coupling $\kappa_{Z\gamma}$ is expected to be measured with an uncertainty of about 10%.[24]

5.3.4. $H \to$ invisible ($H \to$ inv)

While major decay modes of the Higgs boson have been measured with some accuracy, there is enough room for the Higgs boson to decay into[29] a pair of BSM particles such as Dark Matter (DM) candidates. If kinematically accessible, non-interacting DM particles, such as neutralinos in supersymmetry models or graviscalars in models with extra dimensions could manifest themselves as invisible decays of the Higgs boson. Current[5] 95% CL limits on the branching fraction to invisible decays, dominated by the sensitivity in the VBF topology, is about 10%. The irreducible background in this search occurs at 0.1% and arises from $H \to ZZ^{(*)}$ decays where both Z bosons decay into neutrinos. At the HL-LHC, the major challenge in the search for $H \to$ inv stems from the impact of high pileup conditions on the reconstruction of the $E_{\mathrm{T}}^{\mathrm{miss}}$ and its resolution. Feasibility studies[23] in the VH and VBF modes using a variety of $E_{\mathrm{T}}^{\mathrm{miss}}$ threshold project a 95% CL upper limit on $BR(H \to \mathrm{inv}) < 2.5\%$.

6. The Higgs boson self-coupling

The study of the Higgs boson self-coupling represents an important test of the Standard Model, and hence is one of the primary goals of the HL-LHC. Deviations from SM predictions would indicate the presence of new physics beyond this theory. Furthermore, the Higgs boson self-interactions are of primary importance for cosmological theories involving, for example, the vacuum stability and inflation.[5]

Figure 3 shows the theoretical predictions for the total rates at proton-proton colliders with up to $\sqrt{s} = 100$ TeV, see Ref. 30 and references therein. The production cross section at $\sqrt{s} = 14$ TeV is about 39 fb. Figure 4 shows the dependence of the total HH production cross section as a function of the self-coupling λ in units of the SM predicted value. The HH production rate is particularly low for a coupling strength around the SM value, $\lambda/\lambda_{SM} = 1$.

At the HL-LHC, the Higgs boson self-interactions are probed by measuring the HH production rate. The main physics HH final states studied are $HH \to b\bar{b}b\bar{b}$, $HH \to b\bar{b}\gamma\gamma$ and $HH \to b\bar{b}\tau^+\tau^-$. Other channels, such as

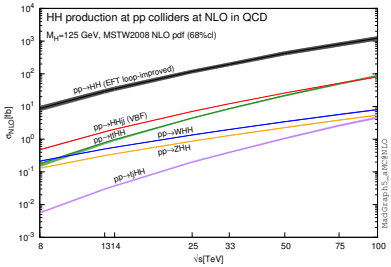

Fig. 3. Total cross sections at the Next-to-the-Leading-Order (NLO) in QCD for the six largest HH production channels at pp colliders. The thickness of the lines corresponds to the scale and Parton Distribution Functions (PDF) uncertainties added linearly.[30]

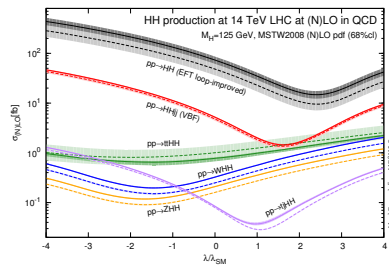

Fig. 4. Total cross section at the Leading Order (LO) and NLO in QCD for HH production channels, at $\sqrt{s} =$ 14 TeV LHC as a function of the self-interaction coupling λ. The dashed (solid) lines and light-(dark-)colour bands correspond to the LO (NLO) results and to the scale and PDF uncertainties added linearly.[30]

$HH \to b\bar{b}W^+W^-$, $HH \to b\bar{b}ZZ$, $HH \to W^+W^-\gamma\gamma$ and $HH \to \tau^+\tau^-\gamma\gamma$ have been also explored. Detailed studies have been reported in the HL-LHC CERN Yellow Report[20] (from now on called "Yellow Report"). In response to the Snowmass 2021 process,[31] new studies and several updates have been produced regarding the HL-LHC projections for non-resonant HH processes, by both ATLAS[24] and CMS[23] Collaborations.

The combined minimum negative-log-likelihoods of ATLAS and CMS projections are shown in Fig. 5. As seen, two minima are found. The first[a] is at $\kappa_\lambda = 1$, as expected for Standard Model. The 68% Confidence Intervals (CIs) are $0.52 \leq \kappa_\lambda \leq 1.5$ and $0.57 \leq \kappa_\lambda \leq 1.5$ with and without systematic uncertainties respectively. The overview of the 68% CI for each channel in each experiment, as well as the combination, is shown in Fig. 6. The 68% CI. for κ_λ are $0.52 \leq \kappa_\lambda \leq 1.5$ and $0.57 \leq \kappa_\lambda \leq 1.5$ with and without systematic uncertainties respectively.

ATLAS has updated the HL-LHC projections for non-resonant HH production in the $HH \to b\bar{b}\gamma\gamma$[32] and $HH \to b\bar{b}\tau^+\tau^-$[33] final states, taking

[a]The presence of a second minimum, located at $\kappa_\lambda \sim 7$, can be mostly explained by the result of the $HH \to b\bar{b}\tau^+\tau^-$ analysis. At κ_λ larger than 1, the HH production cross section increases with increasing κ_λ, and at the same time the signal acceptance decreases, leading to a similar shape to the $\kappa_\lambda = 1$ signal. Together, the degeneracy of the second minimum, originating mainly from the $HH \to b\bar{b}\tau^+\tau^-$ channel, is largely removed by the result of the $HH \to b\bar{b}\gamma\gamma$ analysis. This second minimum of the likelihood can be excluded at 99.4% CL.

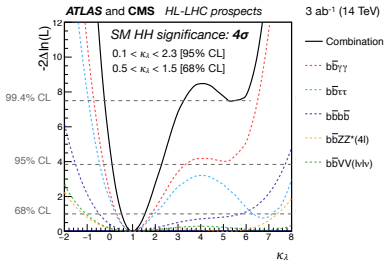

Fig. 5. Minimum negative log-likelihood as a function of κ_λ, calculated by performing a conditional signal+background fit to the background and SM signal. The coloured dashed lines correspond to the combined ATLAS and CMS results by channel, and the black line to their combination. The likelihoods for the channels are normalised to 6000 fb^{-1}.

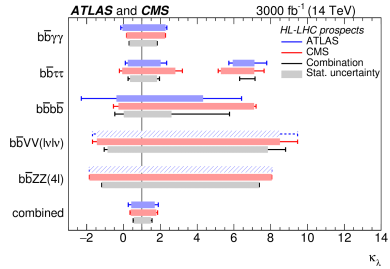

Fig. 6. Expected measured values of κ_λ for the different channels for the ATLAS in blue and the CMS experiment in red, as well as the combined measurement. The lines with error bars show the total uncertainty on each measurement while the boxes correspond to the statistical uncertainties.

advantage of the analysis methodologies which were updated to the latest Run 2 analyses.[34,35]

6.1. *The bbγγ final state*

The $HH \to b\bar{b}\gamma\gamma$ analysis exploits the large $H \to b\bar{b}$ branching ratio in combination with the excellent ATLAS photon resolution, allowing the search for a narrow $H \to \gamma\gamma$ signal in the smoothly falling distribution of the $m_{\gamma\gamma}$ di-photon mass spectrum.

The ATLAS Run 2 analyses studied a categorization based on the output of a BDT discriminant and the modified four-body mass $m^*_{bb\gamma\gamma} = m_{bb\gamma\gamma} - (m_{bb} - 125) - m_{\gamma\gamma} - 125)$ (units in GeV) allowed to increase significantly the sensitivity of this search with respect to previous analyses.

In the Yellow Report, the projection results are obtained using the profile likelihood ratio.[36] Signal and background distributions in the Run 2 categories are first scaled by a uniform scaling factor defined as the ratio between the target integrated luminosity of 3000 fb^{-1} to the Run 2 integrated luminosity (139 fb^{-1}). The change in the center-of-mass energy from $\sqrt{s} = 13$ TeV to $\sqrt{s} = 14$ TeV is accounted for with an additional scaling factor, which depends on the physics process considered. Finally, the projected results in individual analyses are obtained by considering different scenarios of systematic uncertainties.

In the updated projection,[32] the significance of the SM signal ($\kappa_\lambda = 1$) with (without) the baseline HL-LHC systematic scenario increases to 2.2 (2.3) standard deviations (s.d.), an improvement with respect to the values of 2.0 (2.1), with (without) systematic uncertainties, found in the previous study. The combination of all categories results in a 1 s.d. confidence interval on κ_λ of [0.3, 1.9] ([0.4, 1.8]) with (without) systematic uncertainties. This represents again an improvement with respect to the previous projection,[37] which established the 1 s.d. CI for κ_λ to be $[-0.2, 2.5]$ ($[-0.1, 2.4]$).

The CMS Collaboration has also updated its projection using the latest studies of the detector layout in the high-luminosity upgrade and corresponding reconstruction algorithms. In addition to the gluon-gluon fusion process, the new study includes the VBF production mode of HH, which provides a unique access to the HHVV (V = $W^\pm$ or Z bosons) coupling. In the early study this process was neglected. The Vector Boson Fusion process is the second largest production mode of the non-resonant HH production. The study[38] was performed using Monte Carlo samples emulated in the CMS upgrade detector with the DELPHES fast and parametric simulation package tuned for $\sqrt{s} = 14$ TeV and assuming an average pile-up of 200 events per bunch crossing.

The invariant mass distributions derived from the selected photon and b-jets pairs are studied to categorise events according to their signal sensitivities. Figure 7 shows the distribution of the $\gamma\gamma$ invariant mass, $m_{\gamma\gamma}$, for the selected pseudo-data events by this new CMS analysis. The curves correspond to continuum background only (green dashed), total background (continuum + single Higgs boson) (solid blue), and the signal + background (solid red). The signal contribution is shown in solid magenta line at the bottom of the plot.

The expected significance for the inclusive di-Higgs signal is 2.16 s.d. including systematic uncertainties. This is an improvement over the value of 1.83 s.d. reported in the previous study.[39]

6.2. *The $bb\tau^+\tau^-$ final state update*

New b-tagging performance studies expected with the ATLAS detector at HL-LHC were performed by ATLAS since the publication of the Yellow Report, taking into account, in particular, the latest developments in the ITk simulation. The b-tagging performance is not expected to be significantly worse than in Run 2, in spite of the significantly larger pile-up

expected for HL-LHC. The expected b-tagging performance will be very beneficial to the search for the di-Higgs process, in particular, for the study of the $HH \to b\bar{b}b\bar{b}$ and $HH \to b\bar{b}\tau^+\tau^-$ final states. Concerning the $HH \to b\bar{b}\tau^+\tau^-$ final state, the updated projection leads to a signal significance of 2.8 s.d., while the previous extrapolation yielded a signal significance of 2.2 s.d.[33]

Assuming baseline uncertainties, the updated $HH \to b\bar{b}\tau^+\tau^-$ projection provides 1 s.d. Confidence Interval $0.3 \leq \kappa_\lambda \leq 1.9$ and $5.2 \leq \kappa_\lambda \leq 1.9$ which, compared to the previous projection, results in an improvement of 28%. While the full Run 2 search is dominated by statistical uncertainties, the current projection clearly shows that systematic uncertainties will become a limiting factor of the $HH \to b\bar{b}\tau^+\tau^-$ analysis at the HL-LHC.

6.3. *Combination of $HH \to b\bar{b}\tau^+\tau^-$ and $HH \to b\bar{b}\gamma\gamma$ analyses*[40]

ATLAS has also combined the updated projections of the $HH \to b\bar{b}\tau^+\tau^-$ and $HH \to b\bar{b}\gamma\gamma$ final states. The combination of the these updated projections[40] is performed through multiplication of the single analysis likelihoods into a combined likelihood function. The different searches are then fit to the data in order to constrain simultaneously the parameters of interest and the nuisance parameters. The systematic uncertainties of various analyses are correlated following the strategy of Ref. 41.

Values of the negative log-profile-likelihood ratio as a function of κ_λ for various uncertainty scenarios are shown in Fig. 8. If the baseline scenario is assumed, the combination of $HH \to b\bar{b}\tau^+\tau^-$ and $HH \to b\bar{b}\gamma\gamma$ yields a significance of 3.2 s.d. This result is an improvement on the projection presented by ATLAS in the Yellow Report and in subsequent updates, in particular with respect to the analysis where ATLAS combined the projections for the $HH \to b\bar{b}b\bar{b}$, $HH \to b\bar{b}\tau^+\tau^-$ and $HH \to b\bar{b}\gamma\gamma$ final states,[42] where a significance of 2.9 s.d. was estimated.

Combining, the 1-standard deviation confidence intervals on κ_λ are found to be in the interval [0.5, 1.6] in the baseline scenario and [0.6, 1.5] without systematic uncertainties. These intervals show an improvement in sensitivity with respect to the previous projection[42] which reported a 1-standard deviation CI at [0.25, 1.9] ([0.4, 1.7]) with (without) systematic uncertainties.

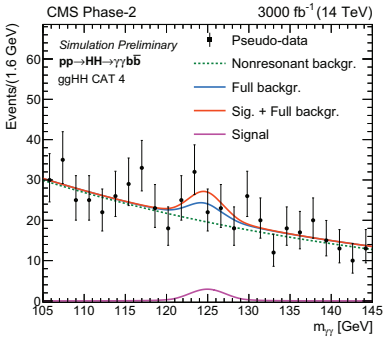

Fig. 7. Distribution of the photon pair invariant mass $m_{\gamma\gamma}$ for the selected pseudo-data events (black points) corresponding to $\mathrm{L} = 3000\ \mathrm{fb}^{-1}$ along with the expectations as estimated from the simulation.

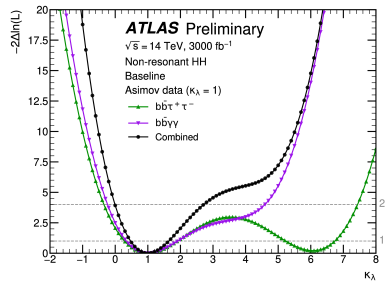

Fig. 8. Negative log-profile-likelihood ratio as a function of κ_λ projected to 3000 fb^{-1} and $\sqrt{s} = 14$ TeV, assuming Standard Model Processes ($\kappa_\lambda = 1$) and assuming the four uncertainty scenarios described in the Yellow Report. Dashed horizontal lines correspond to 1 s.d. and 2 s.d. confidence intervals.

6.4. *The $t\bar{t}HH$ final state and other HH final states*

The production of a pair of Higgs bosons in association with a $t\bar{t}$ pair offers the possibility to explore the interplay between the HH and the $t\bar{t}H$ measurements. This process is also highly sensitive to potential BSM contributions. A preliminary study of this process has been carried out by CMS.[23] In this study, the analysis is based on the reconstruction of events with two Higgs boson decaying each to b-quark pairs, and semileptonic decays of the top-antitop quark pair, which leads to final states with a single lepton, multiple jets, multiple b-jets and moderate missing transverse momentum. The results of this prospect study shows that an upper limit to the $t\bar{t}HH$ production cross section of $3.14^{+1.27}_{-0.9}\times$ *SM prediction* (0.948 fb^{-1}). CMS performed a di-Higgs search study also in the $HH \to W^+W^-\gamma\gamma$ and $HH \to \tau^+\tau^-\gamma\gamma$ channels, which benefits from the sensitive $H \to \gamma\gamma$ process and provides a clean and distinguishable signature. Combining all these final states, the expected significance for signal is 0.22 s.d., including systematic uncertainties at integrated luminosity of 3000 fb^{-1} at the HL-LHC.

6.5. *Summary of the projected precision on self-coupling*

Table 1 shows a summary of the signal significancy of HH final states produced by prospects studies performed by the ATLAS and CMS Collaborations. As seen, the update studies made for the Snowmass process further increased the findings reported in the Yellow Report. The SM double Higgs boson production yield is expected to be measured with a significance greater than 4 s.d. Correspondingly, the Higgs self-coupling modifier κ_λ should be measured with an uncertainty of about 50% by each experiment. The combination of the results from two experiments should yield an uncertainty significantly better than 50%. Further refined studies will consolidate the current projections, and most likely new Deep learning based analyses techniques could increase the possibility of observing (5 s.d.) the Standard Model HH production at HL-LHC, if realised in nature. On the other hand, a statistically significant measurement of $\kappa_\lambda \neq 1$ would be very interesting.

Table 1. Prospects for the signal significance of the HH final states studied by the ATLAS and CMS Collaborations, reported in the CERN Yellow Report. The numbers between [] reports the results presented in the Snowmass paper. The number between () represents a simple combination of the most recent signal significance results available.

HH final state	ATLAS significance (s.d.)	CMS significance (s.d.)
$HH \to b\bar{b}b\bar{b}$	0.61	0.95
$HH \to b\bar{b}\gamma\gamma$	2.0 [2.2]	1.8 [2.16]
$HH \to b\bar{b}\tau^+\tau^-$	2.1 [2.8]	1.4
$HH \to b\bar{b}VV(\mathrm{ll}\nu\nu)$	—	0.56
$HH \to b\bar{b}ZZ(4\mathrm{l})$	—	0.37
$HH \to W^+W^-\gamma\gamma$ + $HH \to \tau^+\tau^-\gamma\gamma$	—	— [0.22]
overall combination: 4.0^{20} ($\sim$4.3)		

7. Summary

The luminosity upgrade of LHC, the HL-LHC, represents a unique opportunity for precision measurements of the Higgs boson properties by ATLAS and CMS. Any significant deviation of these measurements from the Standard Model predictions will indicate presence of new physics beyond SM

at the energy scale of the LHC or colliders proposed for future high-energy physics exploration.

Higgs boson couplings to gauge bosons will be measured with an accuracy of about 2%, while the couplings to the fermions of the third generation and the muons of the second generation will be measured with an accuracy of about 4%. Because of the very small branching ratios, the model-independent measurement of the Higgs coupling to the fermions of the first generation will be very challenging.

The measurement of the Higgs boson mass, an unpredicted parameter in the Standard Model, can be performed at the HL-LHC with an uncertainty of tens of MeV. The direct measurement of the Higgs boson natural width is limited by the energy resolution of muon systems and electromagnetic calorimeters. The $\Gamma_H \simeq 4$ MeV, predicted by Standard Model, can be probed with the study of off-shell Higgs boson production. An uncertainty of 1 MeV (or better) on this parameter is expected at the HL-LHC.

The study of the Higgs self-coupling represents one of strongest physics cases for the HL-LHC programme. The Higgs self-coupling can be studied by measuring the production of Higgs boson pairs. The contribution to the Higgs boson pair production cross section from processes induced by Higgs self-coupling, is very small and thus, large data samples are needed for a precise measurement. At the HL-LHC, the Higgs boson pairs produced by Higgs self-coupling can be observed with a significance of about 5 standard deviations, and the strength of the self-coupling can be measured with an uncertainty of about 50%.

The investigations at the HL-LHC of the Higgs couplings, particularly its self-coupling, will be unique in the world for many decades to come.

8. Acknowledgement

We are grateful to our Funding Agencies support in writing of this manuscript. V.S. is supported by the grant DE–SC0009919 of the United States Department of Energy.

References

1. ATLAS Collaboration, Observation of a new particle in the search for the Standard Model Higgs boson with the ATLAS detector at the LHC, *Phys. Lett. B.* **716**, 1 (2012). doi: 10.1016/j.physletb.2012.08.020.
2. CMS Collaboration, Observation of a new boson at a mass of 125 GeV with

the CMS experiment at the LHC, *Phys. Lett. B.* **716**, 30 (2012). doi: 10.1016/j.physletb.2012.08.021.

3. CMS Collaboration, A portrait of the higgs boson by the CMS experiment ten years after the discovery, *Nature.* **607** (7917) URL https://doi.org/10.1038/s41586-022-04892-x.
4. ATLAS Collaboration, A detailed map of higgs boson interactions by the ATLAS experiment ten years after the discovery, *Nature.* **607** (7917) (Jul, 2022). URL https://doi.org/10.1038/s41586-022-04893-w.
5. R. L. Workman and Others, Status of Higgs Boson Physics in the Review of Particle Physics, *PTEP.* **2022**, 083C01 (2022). doi: 10.1093/ptep/ptac097.
6. G. P. Salam, L.-T. Wang, and G. Zanderighi, The Higgs boson turns ten, *Nature.* **607** (7917) (2022). URL https://doi.org/10.1038/s41586-022-04899-4.
7. ATLAS Collaboration, ATLAS Phase 2 Upgrade Technical Design Reports, URL https://cds.cern.ch/record/2652549.
8. CMS Collaboration, Technical proposal for the phase ii upgrade of the cms detector, URL https://cds.cern.ch/record/2020886. CMS-TDR-15-02.
9. F. Lanni, Overview of the ATLAS HL-LHC upgrade programm; M. Mannelli, The CMS HL-LHC Phase II upgrade program; this book.
10. Addendum to the report on the physics at the HL-LHC, and perspectives for the HE-LHC: Collection of notes from ATLAS and CMS. Technical report, CERN, Geneva (Dec, 2019). URL http://cds.cern.ch/record/2651134, https://arxiv.org/abs/1902.10229.
11. Measurement of the Higgs boson mass in the $H \to ZZ^{(*)} \to 4l$ and $H \to \gamma\gamma$ channels with s = 13 TeV pp collisions using the ATLAS detector, *Physics Letters B.* **784**, 345–366 (2018). URL https://doi.org/10.1016/j.physletb.2018.07.050.
12. A.M. Sirunyan *et al.*, A measurement of the Higgs boson mass in the diphoton decay channel, *Physics Letters B.* **805**, 135425 (2020). URL https://doi.org/10.1016/j.physletb.2020.135425.
13. N. Kauer and G. Passarino, Inadequacy of zero-width approximation for a light higgs boson signal, *Journal of High Energy Physics.* **2012** (8) (Aug, 2012). doi: 10.1007/jhep08(2012)116. URL https://link.springer.com/article/10.1007/JHEP08(2012)116.
14. F. Caola and K. Melnikov, Constraining the higgs boson width with zz production at the LHC, *Physical Review D.* **88** (5) (Sep, 2013). doi: 10.1103/physrevd.88.054024. URL https://journals.aps.org/prd/abstract/10.1103/PhysRevD.88.054024.
15. J. M. Campbell, R. K. Ellis, and C. Williams, Bounding the higgs width at the LHC using full analytic results for $gg \to e^-e^+\mu^-\mu^+$, *Journal of High Energy Physics.* **2014** (4) (Apr, 2014). doi: 10.1007/jhep04(2014)060. URL https://link.springer.com/article/10.1007/JHEP04(2014)060.
16. J. M. Campbell, R. K. Ellis, and C. Williams, Bounding the higgs width at the LHC: Complementary results from $h \to ww$, *Physical Review D.* **89** (5) (Mar, 2014). doi: 10.1103/physrevd.89.053011. URL https://journals.aps.org/prd/abstract/10.1103/PhysRevD.89.053011.

17. CMS Collaboration, Measurement of the Higgs boson width and evidence of its off-shell contributions to ZZ production, *Nature Phys.* **18** (11), 1329–1334 (2022). doi: 10.1038/s41567-022-01682-0.
18. Evidence of off-shell Higgs boson production and constraints on the total width of the Higgs boson in the $ZZ \to 4l$ and $ZZ \to 2l2\nu$ decay channels with the ATLAS detector. Technical report, CERN, Geneva (Nov, 2022). URL `http://cds.cern.ch/record/2842520`.
19. LHC Higgs Cross Section Working Group, C. Potter et al., Handbook of LHC Higgs Cross Sections: 3. Higgs Properties: doi: 10.5170/CERN-2013-004. URL `http://cds.cern.ch/record/1559921`.
20. A. Dainese, M. Mangano, A. Meyer, A. Nisati, G. Salam, and M. A. Vesterinen. Report on the Physics at the HL-LHC, and Perspectives for the HE-LHC. Technical report, Geneva, Switzerland (2019). URL `https://cds.cern.ch/record/2703572`.
21. CMS Collaboration, Search for the Higgs boson decay to a pair of electrons in proton-proton collisions at $\sqrt{s} = 13$ TeV. URL `https://doi.org/10.48550/arxiv.2208.00265`.
22. C. Collaboration, Evidence for Higgs boson decay to a pair of muons, *JHEP.* **01**, 148 (2021). doi: 10.1007/JHEP01(2021)148.
23. Snowmass White Paper Contribution: Physics with the Phase-2 ATLAS and CMS Detectors. Technical report, CERN, Geneva (2022). URL `https://cds.cern.ch/record/2806962`.
24. Snowmass White Paper Contribution: Physics with the Phase-2 ATLAS and CMS Detectors. Technical report, CERN, Geneva (Apr, 2022). URL `https://cds.cern.ch/record/2805993`.
25. C.-W. Chiang and K. Yagyu, Higgs boson decays to $\gamma\gamma$ and $Z\gamma$ in models with Higgs extensions, *Phys. Rev. D.* **87** (3) (2013). doi: 10.1103/PhysRevD.87.033003.
26. C.-S. Chen, C.-Q. Geng, D. Huang, and L.-H. Tsai, New Scalar Contributions to $h \to Z\gamma$, *Phys. Rev. D.* **87**, 075019 (2013). doi: 10.1103/PhysRevD.87.075019.
27. P. Archer-Smith, D. Stolarski, and R. Vega-Morales, On new physics contributions to the Higgs decay to $Z\gamma$, *JHEP.* **10** (2021). doi: 10.1007/JHEP10(2021)247.
28. A. Collaboration, A search for the $Z\gamma$ decay mode of the Higgs boson in pp collisions at $\sqrt{s} = 13$ TeV with the ATLAS detector, *Phys. Lett. B.* **809** (2020). doi: 10.1016/j.physletb.2020.135754.
29. A. Djouadi, A. Falkowski, Y. Mambrini, and J. Quevillon, Direct Detection of Higgs-Portal Dark Matter at the LHC, *Eur. Phys. J. C.* **73** (6) (2013). doi: 10.1140/epjc/s10052-013-2455-1.
30. R. Frederix, S. Frixione, V. Hirschi, F. Maltoni, O. Mattelaer, P. Torrielli, E. Vryonidou, and M. Zaro, Higgs pair production at the LHC with NLO and parton-shower effects, *Physics Letters B.* **732**, 142–149 (May, 2014). doi: 10.1016/j.physletb.2014.03.026. URL `https://www.sciencedirect.com/science/article/pii/S0370269314001828`.

31. Snowmass21: DPF Community Planning Exercise. URL `https://snowmass21.org/energy/start`.
32. Measurement prospects of Higgs boson pair production in the $b\bar{b}\gamma\gamma$ final state with the ATLAS experiment at the HL-LHC. Technical report, CERN, Geneva (Jan, 2022). URL `https://cds.cern.ch/record/2799146`.
33. Projected sensitivity of Higgs boson pair production in the $bb\tau\tau$ final state using proton-proton collisions at HL-LHC with the ATLAS detector. Technical report, CERN, Geneva (Dec, 2021). URL `https://cds.cern.ch/record/2798448`.
34. Search for resonant and non-resonant Higgs boson pair production in the $b\bar{b}\tau^+\tau^-$ decay channel using 13 TeV pp collision data from the ATLAS detector. Technical report, CERN, Geneva (Jul, 2021). URL `https://cds.cern.ch/record/2777236`.
35. ATLAS Collaboration. Search for higgs boson pair production in the two bottom quarks plus two photons final state in pp collisions at $\sqrt{s} = 13$ Tev with the atlas detector. URL `https://arxiv.org/abs/2112.11876` (2021).
36. G. Cowan, K. Cranmer, E. Gross, and O. Vitells, Asymptotic formulae for likelihood-based tests of new physics, *The European Physical Journal C.* **71** (2) (Feb, 2011). doi: 10.1140/epjc/s10052-011-1554-0. URL `https://doi.org/10.1140%2Fepjc%2Fs10052-011-1554-0`.
37. Measurement prospects of the pair production and self-coupling of the Higgs boson with the ATLAS experiment at the HL-LHC. Technical report, CERN, Geneva (Dec, 2018). URL `https://cds.cern.ch/record/2652727`.
38. Prospects for non-resonant Higgs boson pair production measurement in bb$\gamma\gamma$ final states in proton-proton collisions at $\sqrt{s} = 14$ TeV at the High-Luminosity LHC. Technical report, CERN, Geneva (2022). URL `https://cds.cern.ch/record/2803918`.
39. Prospects for HH measurements at the HL-LHC. Technical report, CERN, Geneva (2018). URL `https://cds.cern.ch/record/2652549`.
40. Projected sensitivity of Higgs boson pair production combining the $b\bar{b}\gamma\gamma$ and $b\bar{b}\tau^+\tau^-$ final states with the ATLAS detector at the HL-LHC. Technical report, CERN, Geneva (Feb, 2022). URL `http://cds.cern.ch/record/2802127`.
41. Combination of searches for non-resonant and resonant Higgs boson pair production in the $b\bar{b}\gamma\gamma$, $b\bar{b}\tau^+\tau^-$ and $b\bar{b}b\bar{b}$ decay channels using pp collisions at $\sqrt{s} = 13$ TeV with the ATLAS detector. Technical report, CERN, Geneva (Oct, 2021). URL `https://cds.cern.ch/record/2786865`.
42. Expected b-tagging performance with the upgraded ATLAS Inner Tracker detector at the High-Luminosity LHC. Technical report, CERN, Geneva (Mar, 2020). URL `https://cds.cern.ch/record/2713377`.